Fetal MRI of Urine and Meconium by Gestational Age for the Diagnosis of Genitourinary and Gastrointestinal Abnormalities

Nabeel Farhataziz[1]
Jennifer E. Engels[1]
Ronald M. Ramus[2]
Michael Zaretsky[2]
Diane M. Twickler[1,2]

OBJECTIVE. The purpose of our study was to assess the appearance of the colon and genitourinary tract in fetuses with respect to gestational age with T1- and T2-weighted MRI acquisitions and their applications to abnormalities in these systems.

MATERIALS AND METHODS. Retrospective review of the fetal MRI database was performed to select studies in which both T1- and T2-weighted acquisitions were obtained. The signal characteristics of fluid in the fetal colon and urine in the fetal bladder were evaluated, and gestational age and fetal MRI diagnosis were recorded. A Mantel-Haenszel chi-square analysis was performed to evaluate the relationship of gestational age to MRI signal intensity. In fetuses with suspected colonic and genitourinary abnormalities, an assessment was made about whether the T1-weighted findings added information to the T2-weighted findings.

RESULTS. Eighty fetal MRI studies were reviewed. Forty-three studies showed normal findings, and 37 depicted genitourinary or gastrointestinal abnormalities. The mean gestational age was 27 weeks 6 days. The MRI signal characteristics of urine and meconium became significantly more conspicuous with increasing gestational age (urine bright on T2, $p < 0.001$; urine dark on T1, $p < 0.001$; meconium bright on T1, $p < 0.001$; meconium dark on T2, $p < 0.001$). Of the 37 cases with suspected problems of the gastrointestinal or genitourinary systems, the T1-weighted images added additional information in 23 cases.

CONCLUSION. The appearance of urine and meconium on T1- and T2-weighted images is significantly more apparent with increasing gestational age. T1-weighted images identified meconium in the colon beyond 24 weeks' gestation and aided in the diagnosis of complex abnormalities.

Fetal MRI has been increasingly used as an adjunct to sonography to provide secondary information regarding fetal anatomy, which may alter the antenatal diagnosis and management of the pregnancy [1–5]. The use of ultrafast scanning techniques, such as single-shot fast spin-echo and HASTE sequences, has allowed excellent resolution of fetal anatomy by reducing motion artifact [6]. Most fetal cases referred for secondary MRI evaluation have dealt primarily with CNS and thoracic abnormalities [1, 7–13].

More recently, we and others have used fetal MRI to evaluate the genitourinary and gastrointestinal systems for suspected dysmorphology seen on sonography [2, 14–17]. The appearances of urine and meconium on fetal MRI have been described previously [2, 9, 15–19]. Although there is one report describing the appearance of fetal meconium with respect to gestational age, we are unaware of reports describing the appearance of urine with respect to gestational age and, more specifically, in fetuses at less than 24 weeks' gestation [15]. We have found anecdotally certain appearances of urine in the bladder and fluid in the colon on T1- and T2-weighted images that became more apparent with increasing gestational ages and aided in the diagnosis in many cases by defining which sonolucent structures on sonography represented the colon or genitourinary system. We therefore sought to characterize the MRI appearance of urine in the genitourinary tract and meconium in the colon as a function of gestational age in fetuses without abnormalities in these organ systems. We then attempted to apply these signal characteristics to fetuses with suspected complex genitourinary or gastrointestinal abnormalities with the expectation of improving the diagnostic ability of fetal MRI.

Received April 26, 2004; accepted after revision September 22, 2004.

[1]Department of Radiology, University of Texas Southwestern Medical Center, 5323 Harry Hines Blvd., Dallas, TX 75390-8896. Address correspondence to D. M. Twickler (Diane.Twickler@UTSouthwestern.edu).

[2]Department of Obstetrics and Gynecology, University of Texas Southwestern Medical Center, Dallas, TX 75390-9032.

AJR 2005;184:1891–1897

0361–803X/05/1846–1891

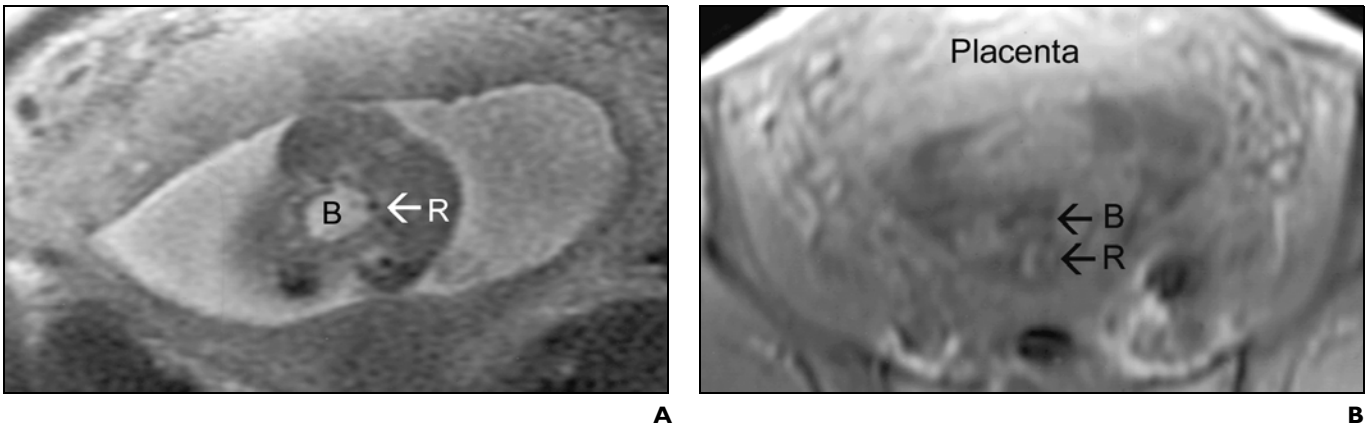

Fig. 1.—MRI of normal genitourinary and gastrointestinal systems in fetus at 22 weeks' gestation.
A, Axial T2-weighted image at level of bladder shows increased signal intensity in bladder (B) and decreased signal intensity in rectum (R).
B, Axial T1-weighted image through bladder (B) shows decreased signal intensity. No bright signal can be identified in expected region of rectosigmoid colon (R).

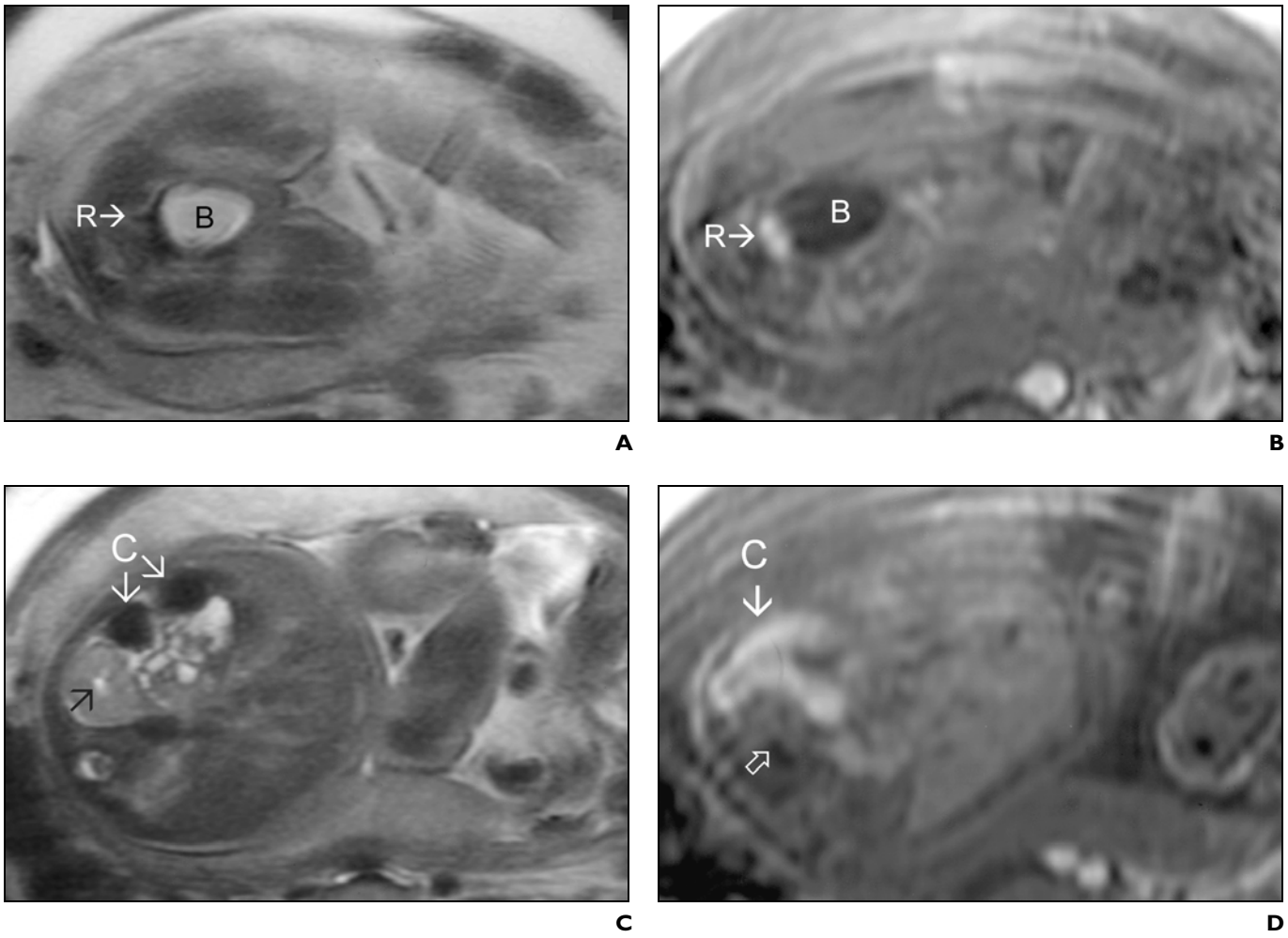

Fig. 2.—MRI of normal genitourinary and gastrointestinal systems in fetus at 30 weeks' gestation.
A, Axial T2-weighted image through level of bladder (B) shows increased signal intensity. Decreased signal intensity is noted in rectum (R).
B, Axial T1-weighted image through level of bladder shows decreased signal in bladder (B) and increased signal in rectum (R).
C, Axial T2-weighted image shows increased signal intensity in left renal pelvis (*black arrow*) and decreased signal intensity in colon in left upper quadrant (C and *white arrows*).
D, Coronal T1-weighted image shows increased signal intensity in colon (C and *solid arrow*) and decreased signal intensity in right renal pelvis (*open arrow*).

TABLE 1 Genitourinary Abnormalities

Gestational Age (wk)	Sonography Findings	MRI Findings	Final Diagnosis
17	Renal agenesis	No additional findings	Renal agenesis
18	Renal agenesis	No additional findings	Renal agenesis
18	Dysplastic pelvic kidney	No additional findings	Dysplastic pelvic kidney
20	Autosomal recessive polycystic kidney disease	Right multicystic dysplastic kidney, left renal hypoplasia	No follow-up
20	Dilated bladder and ureters	Prune-belly syndrome	Prune-belly syndrome
21	Renal agenesis	No additional findings	Renal agenesis
22	Oligohydramnios	Renal agenesis	Renal agenesis
23	Oligohydramnios	Renal agenesis	Renal agenesis
25	Genitourinary vs gastrointestinal anomaly	Horseshoe multicystic dysplastic kidney[a]	No follow-up
27	Oligohydramnios, omphalocele, no bladder seen	Cloacal exstrophy[a]	Cloacal exstrophy
28	Pelvic mass	Urachal cyst[a]	Urachal cyst
28	Pelvic mass	Electrodactyl ectodermal cleft palate[b]	Electrodactyl ectodermal cleft palate[b]
29	Prune-belly syndrome	Prune-belly syndrome with ascites	Prune-belly syndrome
30	Megacystic microcolon, hypoperistalsis	Megacystic microcolon, hypoperistalsis[a]	Megacystic microcolon, hypoperistalsis
30	Adrenal mass	Adrenal hematoma[a]	Adrenal hematoma
31	Multicystic dysplastic kidney	No additional findings	Multicystic dysplastic kidney
31	Bilateral hydronephrosis	No additional findings	Bilateral hydronephrosis
32	Right multicystic dysplastic kidney	Right multicystic dysplastic kidney with ectopic ureterocele[a]	Right multicystic dysplastic kidney with ectopic ureterocele
33	Renal pelvis dilatation	No additional findings	No follow-up
33	Perineal mass	Duplication with ectopic ureterocele[a]	No follow-up
33	Left hydronephrosis, left lower quadrant cyst suspicious for colon	Dilated left renal pelvis with megaureter[a]	No follow-up
37	Abdominal mass	Extraadrenal neuroblastoma[a]	Extraadrenal neuroblastoma
39	Hydronephrosis	Duplication[a]	No follow-up

[a]T1-weighted images provided additional information.
[b]Findings included a median cleft lip, bilateral hydronephrosis, urethral obstruction, ascites, polydactyly, and hydrometrocolpos.

TABLE 2 Gastrointestinal Abnormalities

Gestational Age (wk)	Sonography Findings	MRI Findings	Final Diagnosis
24	Gastroschisis, dilated bowel	Gastroschisis with normal colon	Gastroschisis with colon
24	Cystic mass in left upper quadrant	Mesenteric cyst	No follow-up
25	Congenital diaphragmatic hernia	Congenital diaphragmatic hernia, colon involved[a]	Congenital diaphragmatic hernia, colon involved
26	Congenital diaphragmatic hernia	Congenital diaphragmatic hernia, colon involved[a]	Congenital diaphragmatic hernia, colon involved
26	Fetal pelvic mass	Choledochal cyst[a]	Choledochal cyst
28	Congenital diaphragmatic hernia	Congenital diaphragmatic hernia, colon involved[a]	Congenital diaphragmatic hernia, colon involved
28	Congenital diaphragmatic hernia	Congenital diaphragmatic hernia, colon involved[a]	Congenital diaphragmatic hernia, colon involved
29	Congenital diaphragmatic hernia	Congenital diaphragmatic hernia, colon involved[a]	Congenital diaphragmatic hernia, colon involved
29	Inspissated meconium	No additional findings	No follow-up
29	Twin B with ascites	Meconium peritonitis, ileal atresia[a]	Meconium peritonitis, ileal atresia
30	Fetus in fetu	Retroperitoneal teratoma[a]	Retroperitoneal teratoma
32	Dilated rectum	Normal colon[a]	Normal colon
34	Congenital diaphragmatic hernia	Congenital diaphragmatic hernia, colon involved[a]	Congenital diaphragmatic hernia, colon involved
37	Rectal mass	Normal colon[a]	Normal colon

[a]T1-weighted images provided additional information.

Materials and Methods

Patients and Imaging

For this retrospective study, we reviewed fetal MRI studies performed between January 2000 and January 2003. Before the images were acquired, each maternal patient was counseled about fetal safety issues and written informed consent was obtained as part of an institutional review board–approved study or indicated study.

MRI was performed using a 1.5-T magnet (Signa, GE Healthcare). A torso surface coil was placed around the mother's pelvis and centered over the gravid uterus. No maternal sedation was administered because short acquisition times of the sequences limited fetal motion. A 15-sec localizer three-plane gradient-echo $T2^*$-weighted sequence was performed to plan the orthogonal planes relative to the fetal lie. A single-shot fast spin-echo sequence was used to obtain the T2-weighted images. The parameters used to obtain the images were the following: TR range/TE_{eff} range, 30,000–98,000/50–100; field of view, 30–48 cm (average, 40 cm); matrix, 256 × 128 or 512 × 256; bandwidth, 31.2 or 62.5 kHz; number of excitations, 0.5; interecho spacing, 4.5 msec; and slice thickness, 3–8 mm. A spoiled gradient-recalled acquisition in the steady state (SPGR) was used to obtain T1-weighted images. The parameters were the following: TR/TE, 200/4.2; flip angle, 90°; field of view, 44 cm; matrix, 256 × 128; bandwidth, 20.83 kHz; number of excitations, 1.0; and slice thickness, 5 mm. There were no gaps in either acquisition.

Data Analysis

Retrospective review of the fetal MRI database was performed to select those studies in which both T1- and T2-weighted acquisitions were obtained. Scanning acquisition times, the number of acquisitions, and the total study time were recorded. Gestational age was determined by combined clinical and sonographic information. Specifically, sonography of every fetus was performed before the MR examination, and gestational age was assigned on the basis of the sonographic and clinical information. The studies were reviewed by two examiners together. Initial differences of opinion were not recorded. The studies were identified as either normal or abnormal based on the MRI findings of the genitourinary or gastrointestinal systems. The final diagnosis was made by clinical, surgical, or pathologic follow-up.

The signal characteristics of urine in the fetal bladder and fluid in the fetal colon on both sequences were evaluated. Signal intensity (bright vs dark) was subjectively determined with respect to adjacent muscle. We subjectively evaluated whether there was bright signal in the bladder on T2-weighted sequences but did not quantify bladder fullness. The findings were grouped by gestational age and diagnosis. In fetuses with suspected colonic or genitourinary abnormalities, an assessment was made about whether the T1-weighted findings added information to the T2-

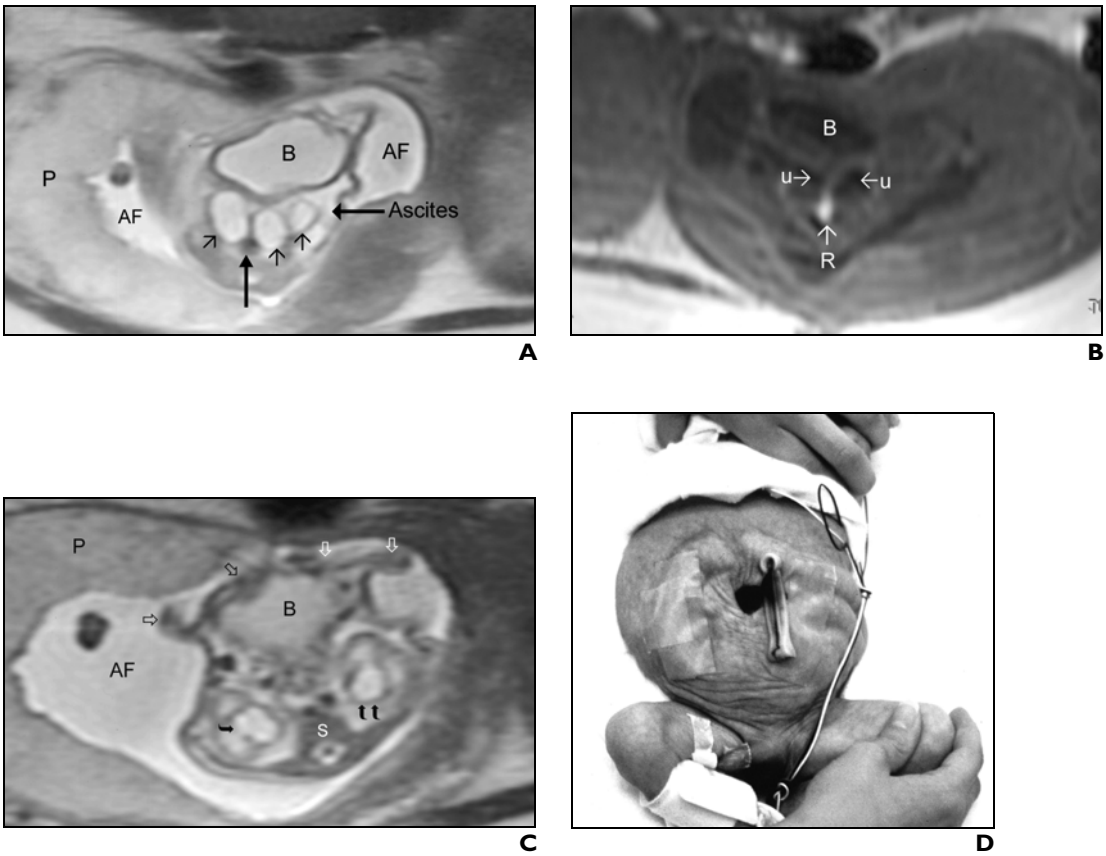

Fig. 3.—MRI of fetus at 29 weeks' gestation with prune-belly syndrome.
A, Axial T2-weighted image at level of bladder shows large bladder (B) and dilated ureters (*short arrows*)—all with increased signal intensity. Amniotic fluid (AF) and ascites also have increased signal intensity. Rectum (*long arrow*) is noted to have decreased signal intensity. Placenta (P) is noted.
B, Axial T1-weighted image through level of bladder shows decreased signal intensity in bladder (B) and ureters (u). Increased signal intensity is noted in rectum (R).
C, Axial T2-weighted image at level of kidneys shows increased signal intensity in renal pelves (*solid arrows*) and increased signal intensity in enlarged bladder (B). Marked contour abnormalities of anterior abdominal wall (*open arrows*) are noted in this case of prune-belly syndrome. Placenta (P), amniotic fluid (AF), and fetal spine (S) are noted.
D, Gross photograph of fetus shows anterior abdominal wall deformity and impressions on anterior abdominal wall secondary to massively dilated ureters.

weighted findings. A Mantel-Haenszel chi-square analysis was performed to evaluate the relationship of gestational age to MRI signal intensity. A p value of less than 0.05 was considered statistically significant.

Results

Using the MRI database between January 2000 and January 2003, we found 80 cases that had both single-shot fast spin-echo and SPGR acquisitions. Scan acquisition times varied from 40 to 90 sec, depending on the number of image slices. An average of 9 acquisitions (range, 5–9) were performed with an average scanning time of 20–30 min. The entire MRI study, including setup, averaged 40 min.

Of the 80 fetuses, 43 had normal findings for the genitourinary and gastrointestinal systems based on MRI and discharge findings. Specifically, none of the fetuses in the normal group had a discharge diagnosis of a gastrointestinal or genitourinary abnormality (Figs. 1 and 2). Thirty-seven of the fetuses had either genitourinary or gastrointestinal abnormalities: 23 genitourinary abnormalities and 14 gastrointestinal abnormalities, which included six diaphragmatic hernias (Tables 1 and 2 and Figs. 3–5). Neonatal outcomes were not available for nine cases in the abnormal group. The mean gestational age was 27 weeks 6 days, with gestational ages ranging from 17 to 39 weeks.

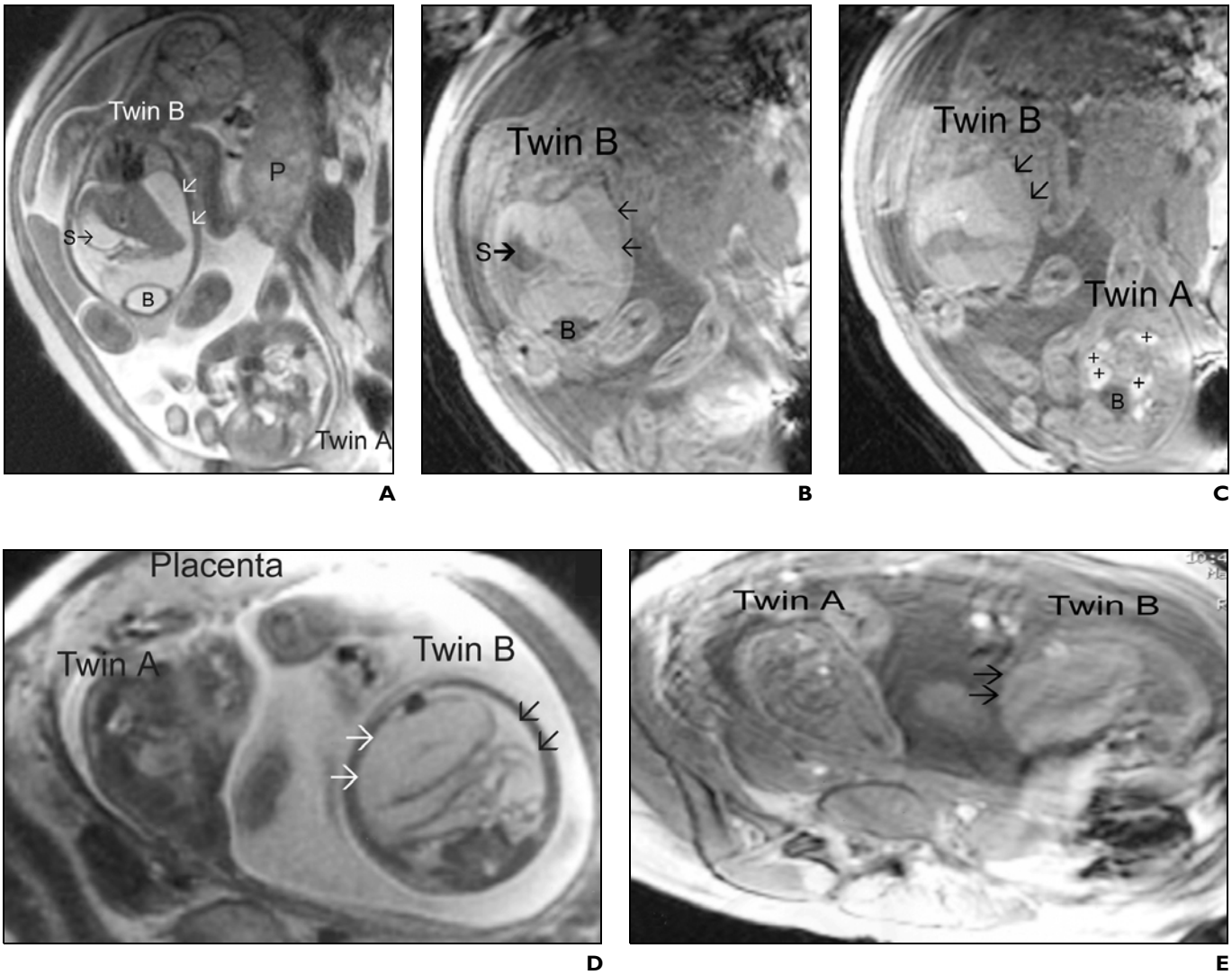

Fig. 4.—MRI of twins at 29 weeks' gestation with meconium peritonitis in twin B secondary to small-bowel atresia. Twin B did not have cystic fibrosis.
A, Coronal T2-weighted image of twin B shows bright signal intensity in bladder (B). Ascites (*white arrows*) is present, consisting of fluid with slightly less signal intensity than bladder and stomach (S). Placenta (P) and twin A are noted.
B, Coronal T1-weighted image of twin B shows ascites (*arrows*) to have intermediate signal intensity, and signal intensity in stomach (S) and bladder (B) is decreased.
C, T1-weighted image of both twins A and B shows twin A to have several normal-appearing loops of colon (+) with increased signal intensity and decreased signal intensity in bladder (B). Twin B is noted to have ascites (*arrows*), which is intermediate in signal intensity; no normal-appearing bright loops of colon are identified in twin B.
D, Axial T2-weighted image of twin B shows dilated loops of bowel (*white arrows*) with intermediate signal fluid. Ascites (*black arrows*) is noted to have slightly higher signal intensity than adjacent bowel contents. Placenta and twin A are noted.
E, Axial T1-weighted image of twin B shows dilated loops of bowel (*arrows*) containing fluid with intermediate signal intensity. No normal-appearing colon with increased signal intensity is identified. Twin A is noted.

The MRI signal characteristics of urine and meconium became significantly more conspicuous with increasing gestational age in both the normal and abnormal fetuses. In 12 of the 22 fetuses at less than 24 weeks' gestation, bright T2 signal was seen in the bladder compared with 54 of the 58 fetuses at greater than 24 weeks' gestation ($p < 0.001$). In nine of the 22 fetuses at less than 24 weeks' gestation, dark T1 signal was detected in the bladder compared with 53 of the 58 fetuses at greater than 24 weeks' gestation ($p < 0.001$). Also, in seven of the 22 fetuses at less than 24 weeks' gestation, bright T1 signal was seen in the colon compared with 57 of the 58 fetuses at greater than 24 weeks' gestation ($p < 0.001$). Finally, in six of the 22 fetuses at less than 24 weeks' gestation, dark T2 signal was detected in the colon compared with 50 of the 58 fetuses at greater than 24 weeks' gestation ($p < 0.001$). Of the 37 cases with suspected problems of either the genitourinary or the gastrointestinal systems, T1-weighted images added additional information in 23 cases, most of which involved discriminating complex genitourinary abnormalities from the colon in fetuses beyond 24 weeks' gestation.

One important note in evaluating the bladder was that except in fetuses with renal agenesis, even with an "empty" bladder, there was still bright signal at the bladder trigone beyond 24 weeks on T2-weighted sequences and that this finding was not dependent on bladder fullness.

Discussion

To our knowledge, ours is the first study comparing the appearance of fetal urine with gestational age. The signal characteristics of fetal urine and meconium in the colon have been described previously, with fetal urine showing a bright signal on T2-weighted images and meconium showing bright signal on T1-weighted images because of its high protein and mineral content [14–18]. Furthermore, the appearance of meconium with respect to gestational age has also been described previously [15]. In our retrospective study, our results agreed with those of previous studies, but the signal characteristics of urine were significantly more apparent with increasing gestational age, especially be-

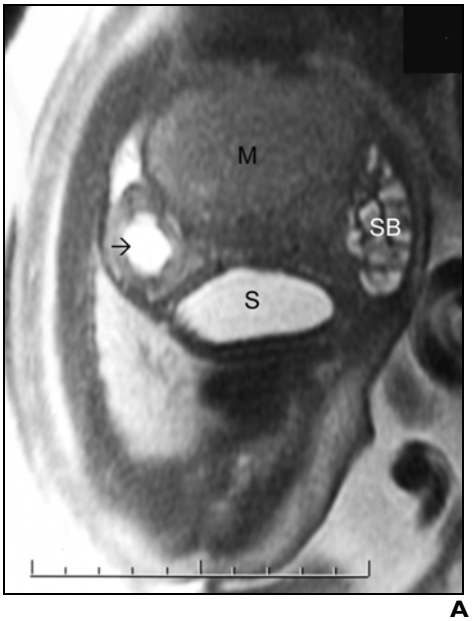

A

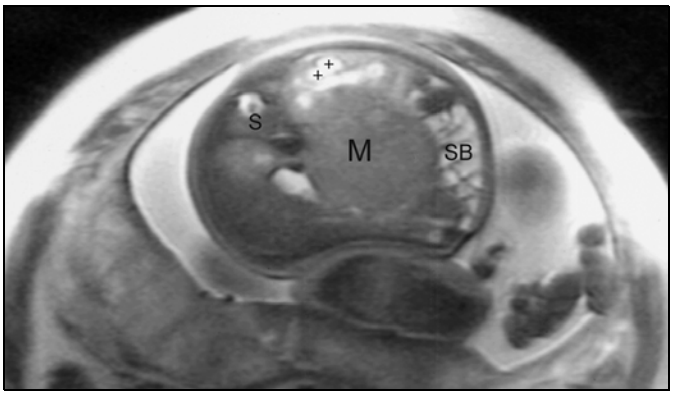

B

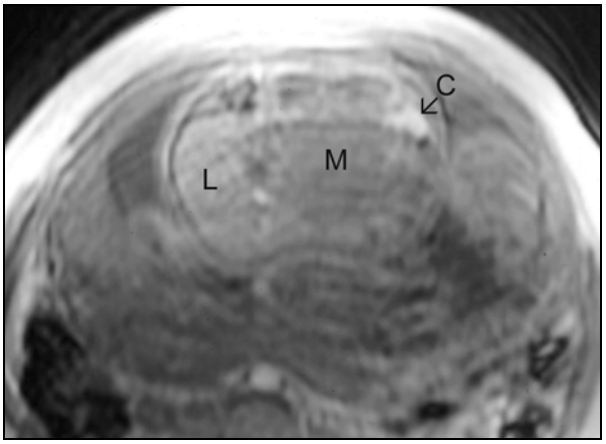

C

Fig. 5.—MRI of fetus at 37 weeks' gestation with extraadrenal neuroblastoma.
A, Sagittal T2-weighted image shows increased signal intensity of fluid in stomach (S) and moderate hydronephrosis of left kidney (*arrow*). Large soft-tissue mass (M) with intermediate signal intensity is seen anterior to left kidney and inferior in relation to stomach. Normal-appearing small bowel (SB) is also visualized.
B, Axial T2-weighted image shows moderate left hydronephrosis (+) and large intermediate-signal-intensity mass (M) anteriorly. Small bowel (SB) and fetal spine (S) are noted.
C, Axial T1-weighted image through level of liver (L) shows large soft-tissue mass (M) that is intermediate in signal intensity. Meconium-filled colon (C) shows increased T1 signal and is lateral to mass.

yond 24 weeks. We also found that T1-weighted images using an SPGR sequence provided additional information in the setting of complex genitourinary or gastrointestinal abnormalities in approximately 60% of the abnormal cases.

In our series of genitourinary abnormalities, imaging in most cases involving fetuses at less than 24 weeks' gestation was performed to identify the kidneys. In these cases, T1-weighted images did not provide additional information because T1-weighted imaging did not aid in determining the presence or absence of kidneys. However, in fetuses at greater than 24 weeks' gestation, identifying the ureters was an important goal and T1-weighted images allowed accurate and reliable discrimination between ureters and colon, thereby providing additional information to decipher complex abnormalities. T1-weighted sequences were also helpful in diagnosing the cases of adrenal hematoma and extraadrenal neuroblastoma by showing blood in the hematoma and fat in the neuroblastoma.

In our series of gastrointestinal abnormalities, identifying meconium in the fetal colon was a primary goal. T1-weighted images resulted in additional information in all but two cases. They were especially helpful in identifying the absence of normal signal of the colon in the cases of meconium peritonitis, megacystic microcolon with hypoperistalsis, and cloacal exstrophy. Also, in the case of gastroschisis with a dilated bowel loop, T1-weighted images identified the dilated bowel to be colon and not obstructed small bowel. In the fetus with a choledochal cyst, T1-weighted images illuminated a potential colon lesion as the choledochal cyst. In the fetus with a retroperitoneal teratoma, T1-weighted sequences were helpful by showing bright signal in the lesion. Finally, T1-weighted sequences were helpful in identifying the presence or absence of colon in the six cases of congenital diaphragmatic hernia to define the severity, although the findings did not necessarily affect counseling or management.

The limitations of this study should be discussed. The retrospective nature of the study may introduce ascertainment bias. In addition, the studies of fetuses at less than 24 weeks' gestation are all genitourinary studies in the abnormal group, so we cannot comment on the benefit of T1-weighted images before 24 weeks' gestation in the setting of gastrointestinal abnormalities. However, we believe T1-weighted images would be helpful in these cases because the rectum is always filled with meconium after 20 weeks and should be easily identified [18]. We did not have neonatal outcomes for nine of the cases with abnormalities including three gastrointestinal cases and six genitourinary cases. Finally, signal characteristics anecdotally are more conspicuous because the organs evaluated become larger and this may play a role regarding increased conspicuity with more advanced gestational age.

In conclusion, we believe our study adds important information to the growing literature of fetal MRI. Specifically, the conspicuity of T1- and T2-weighted findings of urine and meconium in the colon is significantly more apparent beyond 24 weeks' gestation in the fetus and added discriminating information in approximately 60% of the abnormal cases.

References

1. Levine D. Magnetic resonance imaging in prenatal diagnosis. *Curr Opin Pediatr* 2001;13:572–578
2. Breysem L, Bosmans H, Dymarkowski S, et al. The value of fast MR imaging as an adjunct to ultrasound in prenatal diagnosis. *Eur Radiol* 2003;13:1538–1548
3. Twickler DM, Magee KP, Caire JT, Zaretsky M, Fleckenstein JL, Ramus RM. Second-opinion magnetic resonance imaging for suspected fetal central nervous system abnormalities. *Am J Obstet Gynecol* 2003;188:492–496
4. Reichel TF, Ramus RM, Caire JT, Hynan LS, Magee KP, Twickler DM. Fetal central nervous system biometry on MR imaging. *AJR* 2003;180:1155–1158
5. Zaretsky MV, Twickler DM. Magnetic resonance imaging in obstetrics. *Clin Obstet Gynecol* 2003;46:868–877
6. Kubik-Huch RA, Huisman TAGM, Wisser J, et al. Ultrafast MR imaging of the fetus. *AJR* 2000;174:1599–1606
7. Levine D, Barnes PD, Madsen JR, Abbott J, Mehta T, Edelman RR. Central nervous system abnormalities assessed with prenatal magnetic resonance imaging. *Obstet Gynecol* 1999;94:1011–1019
8. Simon EM, Goldstein RB, Coakley FV, et al. Fast MR imaging of fetal CNS anomalies in utero. *Am J Neuroradiol* 2000;21:1688–1698
9. Garel C, Brisse H, Sebag G, Elmaleh M, Oury JF, Hassan M. Magnetic resonance imaging of the fetus. *Pediatr Radiol* 1998;28:201–211
10. Hubbard AM, Adzick NS, Crombleholme TM, Haselgrove JC. Left-sided congenital diaphragmatic hernia: value of prenatal MR imaging in preparation for fetal surgery. *Radiology* 1997;203:636–640
11. Baker PN, Johnson IR, Gowland PA, Freeman A, Adams V, Mansfield P. Estimation of fetal lung volume using echo-planar magnetic resonance imaging. *Obstet Gynecol* 1994;83:951–954
12. Walsh DS, Hubbard AM, Oluyinka OO, et al. Assessment of fetal lung volumes and liver herniation with magnetic resonance imaging in congenital diaphragmatic hernia. *Am J Obstet Gynecol* 2000;183:1067–1069
13. Garden AS, Roberts N. Fetal and fetal organ volume estimations with magnetic resonance imaging. *Am J Obstet Gynecol* 1996;175:442–448
14. Caire JT, Ramus RM, Magee KP, Fullington BK, Ewalt DH, Twickler DM. MRI of fetal genitourinary anomalies. *AJR* 2003;181:1381–1385
15. Trop I, Levine D. Normal fetal anatomy as visualized with fast magnetic resonance imaging. *Top Magn Reson Imaging* 2001;12:3–17
16. Poutamo J, Vanninen R, Partanen K, Kirkinen P. Diagnosing fetal urinary tract abnormalities: benefits of MRI compared to ultrasonography. *Acta Obstet Gynecol Scand* 2000;79:65–71
17. Cassart M, Massez A, Metens T, et al. Complementary role of MRI after sonography in assessing bilateral urinary tract anomalies in the fetus. *AJR* 2004;182:689–695
18. Saguintaah M, Couture A, Veyrac C, Baud C, Quere MP. MRI of the fetal gastrointestinal tract. *Pediatr Radiol* 2002;32:395–404
19. Colletti PM. Computer-assisted imaging of the fetus with magnetic resonance imaging. *Comput Med Imaging Graph* 1996;20:491–496